Journal of Materials Chemistry B

Accepted Manuscript

ROYAL SOCIETY OF CHEMISTRY

www.rsc.org/materialsB

Biological Materials and Molecular Biomimetics – Filling up the Empty Soft Materials Space for Tissue Engineering Applications

Ali Miserez* (1,2), James C. Weaver (3), and Ovijit Chaudhuri (4)

(1) School of Materials Science and Engineering, Nanyang Technological University, Singapore.
(2) School of Biological Sciences, Nanyang Technological University, Singapore.
(3) Wyss Institute for Biologically inspired Engineering, Harvard University, Cambridge, MA, USA.
(4) Department of Mechanical Engineering, Stanford University, Stanford, CA 94305, USA.

* Author for correspondence: ali.miserez@ntu.edu.sg

Abstract

An extensive range of biomaterials, frequently derived from extracellular matrix (ECM) proteins or other natural biopolymers, have been developed for biomedical applications. Their mechanical response, a key requirement for regenerative medicine, is often stiff but exhibits low extensibility (*e.g.* silk), or inversely, is compliant with higher strain to failure (*e.g.* elastin). While synthetic biocompatible materials exhibiting a mechanical response between these boundaries are very rare, several biological materials demonstrate unexpected combinations of these properties. In order to replicate these performance metrics in synthetic systems, a central requirement is to first reveal the molecular design of their constituent building blocks, which has traditionally been an extremely time-consuming task. Here, we highlight the recent application of NextGen sequencing technologies for the characterization of several protein-based natural biopolymers, a technique which circumvents this research bottleneck. Successful molecular biomimcry of these model protein systems could thus have the potential to significantly expand the range of intrinsic material properties available for biomedical applications.

1. Introduction

The last decade has witnessed an increasing interest by researchers from the physical sciences in the exploration of biodiversity as inspiration for materials design strategies. For materials scientists and chemists working in biomimetic and bio-inspired materials synthesis, this attention has largely focused on a multitude of extra-cellular materials from a diverse assemblage of biological systems used for locomotion, protection, or predation [1-3]. The appeal of these biological systems as design inspiration is rooted in the ingenious methods by which these species are specifically adapted to survive and thrive under a wide range of hostile environmental conditions. This interest in biological materials design, however, has led to some misconceptions, principally, that nature

produces superior materials when compared to their anthropogenic counterparts, a notion likely encouraged by their intricate structural designs across multiple hierarchical length scales. It is perhaps more accurate to state that Nature makes things differently, with a more efficient use of energetic resources, and that biological materials are inherently multi-functional [4], with evolutionary pressures guiding the selection of multiple simultaneous local design maxima rather than a single global maximum. From a biomedical perspective, structural or load-bearing materials have received a large share of this research interest since fibrous structures, for example, are critical in applications such as tendon or ligament repair, for sutures, or in wound healing for emergency care [5, 6]. Tissue engineering scaffolds also largely rely on fibrillar materials including, among others, collagen [7, 8], silk [9], fibrin [10], or elastin [11]. In this report, we will provide an overview of the current trends and needs for the use of synthetic and natural biomaterials in biomedical applications, followed by a discussion of some recent discoveries investigating structure-function relationships in non-mineralized structural biological materials (whelk egg capsules, caddisfly silks, and squid sucker ring teeth) and the engineering design lessors that have been learned form their analysis.

2. A brief overview of soft biomaterials for biomedical applications

Polymeric scaffolds have found increasing use in biomedical research, with major applications including drug delivery, tissue engineering, and more recently, *in situ* cell programming (for extensive reviews on these topics, see Peppas *et al*. [12], Lutolf and Hubbell [13], and Kearney and Mooney [14]). In drug delivery, these biomaterials are commonly used for the targeted release of therapeutic agents such as small molecule drugs or protein growth factors. One of the major advantages provided by biomaterial-based delivery is that drug release is highly localized and can directly target a specific region of interest adjacent to the site of implantation, thus permitting lower doses relative to systemic delivery. Additionally, the temporal dynamics of drug release can be precisely tuned through modulation of the physicochemical properties of the scaffold material, so as to optimize drug efficacy. In tissue engineering applications, 3D hydrogels have been utilized as cell-laden carriers to promote tissue regeneration *in vivo*. In practice, a specific cell type of interest can be highly enriched *ex vivo* and delivered via the scaffold carrier directly to the site of injury. The physical and biochemical properties of the scaffold can also be engineered to maximally promote cellular regeneration. Finally, a more recent biomedical application of polymeric scaffolds has been to program cells for a specific targeted activity. For example, scaffolds containing the appropriate biochemical cues can be designed to recruit a specific population of cells into the material, and activate these cells towards a specific set of behaviors [15].

Biocompatible polymeric scaffolds for medical applications can be typically grouped into one of three main classes. One class consists of scaffolds formed from ECM proteins such as fibrin and collagen. These biopolymers are semi-flexible, resulting in gel formation at low concentrations (0.1 -

1% weight/volume is typical) and the elasticity of these gels is highly nonlinear, with significant stiffening at low strains [16]. Fibrin also has the particular advantage of being highly extensible, due to unfolding of coiled-coil domains within the protein under tensile loads [17] and/or via the unraveling of flexible end domains of the fibrinogen constitutive proteins [18]. A clinical application for this class of scaffolds is in the INFUSE bone graft device, in which a collagen sponge is used for sustained delivery of recombinant human bone morphogenetic protein-2, thereby promoting site-specific bone formation [19]. A second class of scaffold-forming materials includes naturally occurring biopolymers such as alginate, hyaluronic acid, agarose, or chitosan. These flexible polymers form high water content hydrogels through either chemical or physical crosslinking at much higher concentrations (typically greater than 1% weight/volume) relative to the semi-flexible protein biopolymer-based gels. In one example application, bone progenitor cells transplanted via degradable alginate hydrogels along with dual growth factors have been demonstrated to induce bone formation *in vivo* [20]. Finally, biomedical scaffolds can be constructed from synthetic polymers, with common examples including polylactide, polyglycolide, or polyethylene glycol [21] polyesters. In the next section, a comparative overview of the mechanical responses of these various classes of biocompatible polymers is presented.

3. Empty spaces in the "soft" materials landscape

The mechanical performance of the chosen material is a critical parameter for regenerative medical applications. Hence, together with their assessment of physico-chemical and biological compatibility, knowledge of their stress-strain characteristics is equally important. When plotting the main types of biocompatible materials used in tissue repair and regeneration on a single tensile stress-strain plot (Fig. 1a, linear scale) a notable feature emerges, specifically that these fibrous materials are mostly segregated into two broad classes (note that the properties shown here were measured under hydrated conditions, which is pertinent for applications in a physiological environment). They are either elastically stretchable with limited ultimate tensile strength (< 1 MPa), as is exhibited by materials such as elastin- and fibrin-based hydrogels, or as in the case of silks, they are stiff and strong, but feature limited extensibility. While native collagen is one exception, appearing somewhere in the middle [22], such properties have not been recapitulated with synthetically processed collagens. Although there has been recent progress in this area of research [8, 23], synthetic collagen fibril synthesis remains a challenging task because it consists of a multi-step and hierarchical assembly process, spanning from the classical triple-helix secondary structure to the nano-staggered arrangement, all of which are important requisites governing the mechanical response of this material [24, 25]. Chitosan biopolymers are mid-range between these upper and lower boundaries, with Young's modulus values in the 1-10 MPa range under hydrated conditions [26, 27] and exhibit a rather limited extensibility of 10-15%. This contrast in mechanical performance is perhaps

better perceived on the log stress-strain representation shown in Fig. 1b. Here it appears rather clearly that between the stiff silks (and even native collagens) and the highly elastic materials and hydrogels, there exists ample room to tailor the structural properties of biomaterials. This material tailorability has clear advantages in cases where such intermediate properties would be required. For example, a central requirement of connective tissues is to bond different tissues that often exhibit significant differences in mechanical properties [28], and this task is best achieved by using materials with stress-strain characteristics ranging between those of the tissues to which they attach. Even more suitable are materials that feature mechanically-graded properties, because smooth gradients can shield the interfaces against stress concentration that are often the sites of mechanical failure [29]. Achieving these macrostructural gradients is easier if the intrinsic properties of the building blocks can be controlled over a few orders of magnitude, since the mechanical gradient can be obtained by spatially varying the volume fraction of the starting materials [30, 31] through a simple composite effect or by manipulating the cross-linking density [32].

Let us consider the simplest case of linear elastic fibers, where the failure energy or work of fracture w_f is given by the relation:

$$w_f = \frac{1}{2} \cdot \varepsilon_f{}^2 \cdot E \qquad \text{Eq. 1}$$

where ε_f is the strain to failure and E is the Young's modulus. Commonly used biomaterials can be placed on a log-log plot with ε_f on the x-axis and E on the y-axis, and guidelines in the spirit of Ashby materials selection charts [33, 34] can be drawn (Fig. 2a). Materials located along a given -(1/2) slope guideline are predicted to exhibit equivalent energy to failure. A striking feature is that biomaterials with elastic moduli in the range 1 – 100 MPa are uncommon, which we will refer to here as the "empty soft materials space" (it should be emphasized that this plot is not meant to represent a comprehensive Ashby selection chart of all biomaterials, but to provide general design guidelines).

There also exist other, more subtle characteristics, which would be useful in applications involving cell and tissue encapsulation. For example, the ability to dissipate mechanical loads can be critical for the protection of delicate cells [35], for artificial fibers used for connective tissue replacement, or in cartilaginous tissue engineering. This property manifests itself on the stress-strain curve as hysteresis upon unloading (schematically illustrated in Fig. 2b); the larger the hysteresis during a loading/unloading curve, the more efficiently the material can dissipate elastic energy. When commonly used soft biomaterials are placed on a hysteresis *vs.* elastic modulus plot, only a few examples exhibit more than 10% of absorption capacity upon unloading. Notable exceptions to this trend are native (hydrated) dragline silks [36] and genetically-engineered titin/resilin hybrid

materials [37]. For the titin/resin synthetic constructs, however, the macro-scale performance has not been evaluated and their mechanical characterization has so far been limited to single-molecule pulling experiments by AFM. More recently, there have also been significant advances in the synthesis of high performance hydrogels [38] that exhibit significantly greater toughness compared to traditional formulations. Such toughened gels (generally referred as "physically cross-linked gels" in the materials selection chart of Fig. 2a) appear to bridge the mechanical property gap between soft tissues and synthetic gels [39]. Interestingly, the underlying nano- and micro-scale toughening mechanisms behind these properties are conceptually similar to those responsible for the unique mechanical response of natural biological materials described in the following section. Based on these observations, there thus exists a large empty soft material parameter space (highlighted in yellow in Fig. 2a) where new materials could be developed.

4. Looking to Nature to fill the void in soft material property space

Over the past several years, we have identified and characterized, across multiple length scales, several intriguing biological materials systems from various species of marine invertebrates that exhibit a wide range of unique properties for potential biomedical applications [30, 40-42], a selection of which are described below. Other research groups have focused their attention on fibrous structures from insects, which are also briefly described.

The oviparous marine snails from the family *Melongenidae*, for example, deposit their eggs within tough and stretchable egg capsules. These capsules are exclusively proteinaceous and exhibit unusual mechanical tensile responses [43, 44]. After an initial linear elastic regime, with an elastic modulus of ca. 50 to 70 MPa, they display a pseudo-yield behavior up to 70% strain. Upon further stretching, the capsular materials significantly strain-harden and can be deformed up to 170%. When the external load is released, the material recovers its initial length. In comparison to most other elastomeric materials, however, a high amount of elastic energy is internally absorbed as witnessed by the high hysteresis during a full load/unloading cycle. In other words, the egg capsule is able to absorb a large fraction of the total elastic energy stored during loading. If we place the egg capsule on the ε_f vs. E materials selection chart (Fig. 2a, purple box), we see that they are ideally located within the empty materials space described in the previous sections. In addition, on an energy absorption *vs*. modulus chart, the egg capsule again features a combination of properties unmatched by any synthetic polymer or soft material (Fig. 2c). Clearly, our ability to duplicate such properties would expand the range of existing materials properties for a wide range of regenerative medical applications.

What is the source of these unusual properties? At the micron-scale, the egg capsule is composed of fibers, which in a species-specific manner, are arranged either in an orthotropic or random fashion [41, 45]. These fibers are made of smaller, nano-scale units which feature an axial staggered arrangement of 100 nm, which is reminiscent of the 67 nm staggered organization of collagen triple helices [45, 46]. *In-situ* tensile testing performed in conjunction with Wide-Angle X-Ray diffraction [41] and confocal Raman imaging [46] have shown that the key features governing the egg capsule tensile behavior are conformational changes of the protein backbone under mechanical stress. The egg capsule micro-fibers are essentially made of coiled-coil proteins in the unstretched state and undergo a conformation transformation into axially-aligned extended β-sheet-like structures during stretching. This solid-state phase transition behavior has recently emerged as a common theme in a variety of biomacromolecules [47], including fibrin [48], intermediate filaments [49], and myosin II [50].

Another class of biological fibers recently reported by Stewart and co-workers that exhibit a similar mechanical response to the whelk egg capsules are the larval caddisfly silks [51, 52], which are used to glue together solid particles into a protective casing. The tensile response of caddisfly slik is characterized by an initial linear regime up to ~ 5% strain, with a Young's modulus of ca. 80 MPa. Like the whelk egg capsules, a yield plateau is then observed up to ca. 20% strain, which is followed by strain hardening until failure at 100 to 170% strain. Upon unloading, a high hysteresis is observed and is accompanied by a large irreversible strain, which is, however, restored after 15 minutes at rest. Plotting caddisfly silk on the same Ashby plots (Fig. 2, red box), reveals that its performance metrics position it near the marine snail egg capsule, but with an even higher mechanical hysteresis (Fig. 2c). However, in comparison to the whelk egg capsule, the reversible elongation is not instantaneous. Structure/property relationship studies of caddisfly silk with solid-state NMR and XRD have indicated that anti-parallel β-sheets are a key contributor to the stiffness and strength of the fibers [51], which is reminiscent of spider silks. An additional striking feature of caddisfly silk is their substantial post-translational phosphorylation as well as the presence of Ca^{2+} ions, which were shown by FTIR to form Ca^{2+}-phosphate complexes. Upon chelation of Ca^{2+} with EDTA, the mechanical properties (stiffness, yield, and ultimate strength) are dramatically reduced along with a concomitant reduction in β-sheet content. These characteristics, however, can be largely restored following re-incubation with Ca^{2+}, thus strongly suggesting that phosphate/Ca^{2+} complexation plays a key role in enhancing their mechanical response [52] and in stabilizing the β-sheets.

Another promising model biopolymer we have recently characterized comes from the arms and tentacles of decapodiform cephalopods (squids and cuttlefish) such as the Humboldt (or Jumbo) squid, *Dosidicus gigas*. Jumbo squid are swift, agile, and aggressive predators that use their

muscular tentacles and arms during prey capture and handling. The tentacles and arms are lined with hundreds of suckers, each of which contains a rigid ring-like structure from which robust triangular teeth protrude. Despite being entirely proteinaceous, these sucker ring teeth (SRT) are as hard and stiff as some of the strongest synthetic polymers [53] with a Young's modulus ranging from 6 to 8 GPa under dry conditions and 2 to 4 GPa when in a hydrated state. The cross-sectional variation in modulus is correlated to the presence of nanotubules oriented parallel to the long axis of the teeth. Perhaps, even more remarkable, is the fact that there are no inter-chain covalent interactions within the teeth. Instead, SRT are assembled into large supramolecular networks containing a high volume fraction of nano-confined β-sheets and held together primarily through hydrogen bonding interactions [54]. The intriguing absence of inter-chain chemical linkages can be exploited during the synthetic processing of the SRT proteins. As a result, SRT are soluble under mildly acidic conditions, can be reversibly melted by simple heating just like a thermoplastic polymer, and in turn, can be molded into complex shapes across multiple length scales, with β-sheets spontaneously forming upon solidification or solution evaporation [55]. The design lessons obtained from investigating this thermoplastic-like behavior and water-based processability has the potential to provide "green" approaches for the synthetic fabrication of high-performance protein-based polymers for regenerative medical applications where very high load-bearing properties are required.

Towards our goal to duplicate these systems, a central requirement relates to the need to elucidate the genes that encode their constitutive proteins. While historically such efforts have been extremely time-consuming, there have, however, been exciting developments in the recent years that have the potential to dramatically reduce the time constraints needed to sequence and clone such intriguing biomacromolecules, the details of which are described in the following section.

5. Molecular biomimetics: Structure-properties relationships at the protein sequence level

5.1 Next Gen sequencing for Biological Structural Materials

A central issue –and a major bottleneck in the design of biomimetic materials– has been the time required for obtaining full-length protein sequences of interest. For example, the development of mussel-inspired adhesives, arguably one of the best success stories of biomimetics, took decades and was completely dependent on the discovery of the "adhesive" dihydroxyphenylananine (DOPA) side chain modification [56] and on the elucidation of the primary amino acid sequences of these natural protein-based glues [57-61]. These characteristics later inspired a wide range of chemical strategies for the development of catechol-based synthetic polymers for biomedical applications [62, 63], including those based on the clever use of dopamine chemistry [64]. Likewise, the development of

genetically engineered silk-like fibers fully relied on the sequencing of silk genes. But while key silk secondary structural motifs were first elucidated in the 1950s [65], it wasn't until more than 30 years later that the first partial silk protein sequence was obtained by Xu and Lewis [66], followed a few years later by partial sequencing of other silk genes [67-69]. Of course, this understanding has been intimately linked to parallel advances in molecular cloning technologies, since the discovery and characterization of novel proteins from extracellular biological materials was intrinsically limited by sequencing bottlenecks. There have also been other limiting factors that have slowed progress on this front. First, proteins from structural biological materials are often difficult to extract owing to their intrinsic chemical stability. They are often covalently cross-linked [70-72], precluding their isolation with common extraction buffers and also tend to form insoluble aggregates. Furthermore many contain post-translation modifications –often unknown- which are critical for their proper function in the extra-cellular environment. To further complicate this situation, the elucidation of these modifications is not straightforward and cannot be obtained through standard molecular cloning. Second, while an increasing number of genomes have been sequenced in recent years [73] there is still very limited genomic information for many interesting model systems that are currently being explored in the biomimetics materials community. In turn, obtaining full-length sequences of novel proteins though either direct N-terminal, C-terminal, and internal fragmentation sequencing or through the use of more traditional molecular biological techniques is perceived as a challenging endeavor, and is thus not often undertaken in the bioinspired materials community.

With remarkable advances achieved in the past few years with Next Generation Sequencing Technologies [74-76], many of the constraints described above have been lifted. In light of these recent discoveries, we have employed Next Generation RNA-sequencing (RNA-seq) in the context of biological materials characterization [55]. This approach involves the following steps, summarized in Fig. 3. The transcriptome of a specific tissue can be rapidly obtained from mRNA extraction and isolation, from which a cDNA library can be generated. Transcripts are then assembled using bioinformatic tools such as the Trinity software suite [77], which assembles transcripts without a reference genome library. In parallel, proteomic analyses of the tissue or glands secreting the protein of interest are conducted with classical and modern proteomic tools, including amino acid analysis (AAA), *N*-terminal sequencing, or high throughput tandem mass spectroscopy (as a side note, it is interesting to mention that traditional analytical techniques such as AAA or Edman-based sequencing, which have tended to vanish from Life Sciences laboratories in the past decade, have proved extremely useful in order to mine biological material transcriptomic libraries, especially when looking for novel proteins). Genes of interest are then obtained by probing the transcriptome library with the proteomics data, including protein amino acid composition, isoelectric point and molecular weight, as well as *N*-terminal and internal sequence information. Once candidate transcripts have been identified, standard PCR techniques may still be needed in some cases to confirm the final full-

length sequences, especially for the highly repetitive sequences that are common in structural proteins. This step, however, is extremely accelerated through prior knowledge of the candidate transcripts and in our experience, has not led to any ambiguities or major difficulties in obtaining the genes of interest.

Using this approach, we have been able to successfully obtain full-length sequences from our targeted model systems. Other groups have also recently made use of similar approaches to sequence caddisfly silks [52] or the underwater adhesives from barnacles, flatworms, and sea stars [78-80], indicating an increasing awareness towards this integrative research platform. Significantly, and using these approaches, most genes of interest from a given model system have been sequenced with only a few months of work. Until recently, such critical sequence information –which is key for subsequent synthetic biomimetic efforts through protein engineering [81, 82] or peptide synthesis– would have typically taken many years of tedious molecular cloning work, often to obtain only a few genes of interest [83]. Overall, this research platform is extremely promising since it permits the genes from a newly identified model system to be rapidly sequenced, significantly reducing or eliminating the many hurdles faced when tackling novel protein sequencing from natural biological materials.

5.2 Sequence analysis of model tissues

We now return to the model systems described in Section 4 and briefly describe the key molecular features gleaned from the sequencing of their constituting proteins.

Whelk Egg Capsules: Coiled-coil-based bioelastomer

Analysis of the full-length sequences of egg capsule proteins (ECPs) with coiled-coil predictor tools [84, 85] have identified the presence of long coiled-coil domains within the ECPs from various marine snail species [45, 86]. These predictions were confirmed by Circular Dichroism (CD) measurements on both crude and purified ECPs. In addition, self-assembly experiments followed by MALDI-TOF provided evidence for oligomer assemblies of heptad repeats, the hallmark of coiled-coil structures. These coiled-coil repeats were predicted to encompass at least 50% of the ECP total length, with a central helical rod flanked by non-helical head and tail domains. The overall ECP sequence design bears some similarity with intermediate filaments (IFs), which play an important structural role in the function of the cellular cytoskeleton [87]. Other subtleties common to IFs include the presence of localized irregularities in the heptad repeats, which have been predicted to act as nucleation sites for the α-to-β transition of IF coiled-coils [88]. Previous computational studies have predicted that a minimum requirement of 29 amino acids in the heptad repeat domains is required for the α-to-β transition to occur [49], a condition which is met by all of the predicted heptad repeat

domains of the ECPs. The presence of long coiled-coils rods in ECPs thus appears to be a key molecular requirement for the α-to-β transition of constitutive ECPs. Notable differences in the heptad repeats are also observed when comparing ECPs with libraries of other coiled-coil proteins. Specifically, ECPs contain a relatively high number of Gly residues within the hydrophobic core and a lower content of aromatic residues compared to other well-studied coiled-coil sequences. An increased abundance of small Gly at the expense of bulky aromatic residues may increase chain dynamics, which is likely to be helpful in facilitating α-to-β phase transformations. Such comparative analyses of structural biological material sequence designs across related species [45] can be rapidly performed using RNA-seq, and provide important information for subsequent biomolecular engineering studies by exploiting both convergence and divergence in the sequence designs. Convergence indicates which domains are key for the function, whereas divergence (with similar macroscopic properties, such as in egg capsule proteins from various species) teaches us that there exists a level of design flexibility in the creation of recombinant biomimetic analogs. Overall, these data add naturally-occurring heptad repeats to the repertoire of coiled-coil proteins [89, 90], whose key function in the natural system is in highly elastic, energy absorption, and load bearing applications. The possibility of filling up the gaps displayed in Fig. 2 in the soft material property landscape may thus be obtainable within a reasonable timeframe using recombinant coiled-coil egg capsule proteins.

Caddisfly silks: Phosphorylated underwater fibrous adhesives

The primary structure of caddisfly silks consists of relatively short N- and C-terminal domains flanking a much longer central domain [52]. While the full-length sequence has not been obtained because of the extremely repetitive nature of the central domain, the latter is mostly comprised of three types of conserved subrepeats that are irregularly distributed along the protein. While each repeat is enriched in Arginine (Arg), one domain is very Gly-rich, whereas the two other domains contain a high amount of Ser. One of these Ser-rich domains exhibits a highly conserved sequence with multiple poly-Ser peptides. Furthermore, a striking feature of the caddisfly silk is the high degree of phosphorylation of Ser residues (as detected by mass spectroscopy of tryptic peptides) in each subprepeat. Molecular dynamic simulations indicate that the conserved Ser-rich sequence, which is also phosphorylated, is likely to form a β-hairpin structure that is stabilized by Ca^{2+} ions [52]. Thus, the phosphorylation modification appears to be a key feature of the fiber mechanics, which could perhaps prove challenging to duplicate in future biomimetic efforts through protein engineering.

Sucker ring teeth (SRT): A nanoconfined β-sheet reinforced supramolecular network

Transcriptome assembly and sequence analysis have shown that SRT are assembled from a protein family called "suckerins" that are highly modular with a general di-block copolypeptide-like architecture. The first type of repetitive module (M1) is enriched in Ala, His, and Thr, whereas the second type (M2) is Gly-rich with a significant amount of Tyr. These modules are further divided into smaller-scale building blocks, with a predominance of poly-Ala repeats intervened with Thr in the first type of module, and peptides such as GGY and GGLY in the second module type. Intriguingly, the closest structural biological material systems to the suckerin in terms of molecular design are the silk proteins [83]. Silk mechanical performance is well-known to arise from the presence of β-sheet crystals that strengthen the network [91, 92] and similarly, a high abundance of β-sheets was also identified in SRT by Raman and FTIR spectroscopy measurements [55]. Using a comparative approach where transcriptomes of sucker tissues from three cephalopod species were assembled and analyzed [54], it was further revealed that the suckerin protein family displays a conserved bi-modal architecture across these species in the form Pro-[M1]-Pro-[M2], with a conserved number of amino acids within the [M1] modules that are flanked by Pro residues. Synchrotron Wide-Angle X-ray Scattering (WAXS) indicated that β-sheets in SRT are around 2.5 to 3.5 nm in size. Given that [M1] modules are enriched in β-sheet favoring residues and that Pro is a well-known β-sheet disruptor, an important implication was that [M1] modules form nanoconfined β-sheets whose size is constrained by the precise placement of the Pro residues. Concomitant nanomechanical and Raman spectroscopy of SRT cross-sections under conditions that disrupted hydrogen bonding and β-sheet formation showed that the nanoconfined β-sheets are directly responsible for enhancing the mechanical strength of SRT. Together, these data provide novel molecular designs that can be fully duplicated into full-length proteins through recombinant expression. Alternatively, they can be used as modular peptides for incorporation into the backbone of other known load-bearing proteins or as side-chain functionalized units of hybrid polymers.

Silk has generated intense interest in recent years, with many successfully demonstrated biomedical and engineering applications[9, 93, 94]. One challenge with silk processing, however, is the required use of rather harsh solvents in order to solubilize native and high molecular-weight recombinant silks. Furthermore, owing to their extremely high molecular weights (>400 kDa) and the heavy bias towards Gly and Ala, expression of full-length recombinant silk proteins remains challenging, although there has also been recent progress on this front [95]. In comparison, the recombinant expression of full-length suckerin proteins was not met with major technical difficulties, and just like the native SRT proteins, recombinant SRT proteins can be processed from aqueous solutions at various length scales and into various shapes, while spontaneously forming a high percentage of β-sheets. Sequence analysis of the SRT proteins has also revealed the regular

placement of tyrosine, which was exploited to tune the mechanical properties in wet conditions over 2-orders of magnitude by forming di-tyrosine cross-links using a straightforward photo-activation method [55]. As illustrated in a materials selection chart (Fig. 4), the combination of hardness and modulus of SRT proteins can match or even exceed those of the strongest synthetic polymers. Interestingly, the inspiration for the di-tyrosine cross-linking came from another natural bioelastomer, namely resilin [96] from insect wings, which had previously been shown to contain di-tyrosine and whose properties can be artificially mimicked through photo-induced cross-linking [97].

6. Towards the incorporation of bio-inspired modular peptides for the design of structural biomedical materials

The identification of full-length sequences from load-bearing, elastomeric, self-healing, and other intriguing biological model systems provides completely new libraries of biomimetic proteins and peptides that can readily be combined or fused with previously available proteinaceous materials [81], or grafted into other hybrid systems such as those based on synthetic polymers or polysaccharides. As described in the previous sections, this molecular toolbox thus has the potential to facilitate the development of novel biopolymeric material systems that offer combinations of properties not currently available in existing materials. Using these approaches, we come one step closer to filling the “empty spaces” present in the soft materials landscape depicted in Fig. 2, not only in terms of structural performance but also with the capacity to incorporate novel properties such as stimuli-responsiveness, controlled degradation [98], or anti-oxidative activity [61].

One recent trend, for example, has been to combine different classes of polymers to generate composite matrices with enhanced mechanical or biological properties. Examples of this approach include the fabrication of interpenetrating networks of covalently cross-linked acrylamide and ionically cross-linked alginate gels that are both tough and highly extensible [99]. In a second example, interpenetrating networks of reconstituted basement membrane matrix and alginate have been used to modulate matrix stiffness independent of ligand density [100]. These types of multi-phasic biopolymeric constructs could be especially relevant in the field of cartilage tissue engineering due to cartilage’s low intrinsic capacity to heal and the continuous, long term, and relatively high dynamic stresses (~20 MPa) [101] that this tissue experiences [102]. Compared to natural cartilaginous tissues, however, engineered cartilage equivalents generally exhibit a nearly 10-fold reduction in mechanical performance in terms of their toughness and tensile and compressive moduli [103]. While much still remains to be learned regarding the synthesis methods to custom-tailor the mechanical properties of biomedical materials that function as cartilage replacements, recent advances in the use of blended gels of fibrin-alginate have been used to form fibrocartilage tissue equivalents *in vitro* that exhibit greater extensibility, while still possessing the capacity to promote

chondrogenesis and cartilage matrix production by mesenchymal stem cells [104]. Recently developed tough hydrogels (displayed in the materials selection chart in Fig. 2a) also exhibit promising mechanical properties as cartilage replacement materials, with Young's moduli under hydrated conditions ranging from 0.3-0.4 MPa [105] to greater than 1 MPa [39]. On the other hand, however, if we consider the lessons learned from investigating structural biological materials, marine snail egg capsules, for example, exhibit a mechanical response that could potentially be highly suitable for such applications, including a high elastic modulus of 50 to 70 MPa combined with a fully reversible extensibility of 150% (a combination of properties that exceeds that of traditional tough synthetic elastomers [106]), while simultaneously exhibiting high mechanical energy absorption and a high fatigue resistance [44].

Tough hydrogels typically rely on a double cross-linked network as a primary toughening mechanism, where weak "sacrificial bonds" such as hydrogen bonds provide energy dissipation, while a second covalently cross-linked (and stronger) network is responsible for the load bearing capability and increased elasticity. Conceptually, it is interesting to note that the mechanical properties of marine snail egg capsules can also be attributed to a double-network system: during mechanically-induced unfolding of the coiled-coil rods, breaking of *intra*-chain hydrogen bonds that stabilize the coiled coil parallel to the rod axes occur. As the strain is further increased, transient, *inter*-chain hydrogen bonds within the extended state of β-sheet-like domains are formed. The intra-chain bonds reform almost instantaneously upon unloading, similar to hydrogen bonds within ureidopyrimidinone (UPy) segments reported by Guo *et al* [105] and to ionic bonds in ampholyte-based hydrogels [39]. The elasticity and improved load-bearing properties, on the other hand, are largely attributed to the presence of Lysine-derived covalent cross-links which render the egg capsule not only mechanically, but also highly chemically stable. Exhibiting a nearly 50-fold increase in modulus compared to the stiffest known synthetic gels, the impressive mechanical properties of the egg capsules are likely related to their low water content as well as the intrinsically stiffer nature of the coiled-coil structural motif [107, 108]. Tough hydrogels, on the other hand, are more extensible (ranging from 500 to 1000%) vs. ca. 150% for the egg capsules. Since the work of fracture scales linearly with E and exhibits a power of two dependence with ε_f (Eq. 1), the egg capsules and tough hydrogels are found along roughly the same energy to failure guideline in Fig. 2a. Thus, in terms of fracture energy, the lower strain to failure of the egg capsules is compensated by their high moduli. A useful target for future development would be to tailor the properties between these boundaries, perhaps by creating hybrid systems that are based on both synthetic and natural strategies of the respective materials. We envision that either full-length recombinant proteins or shorter modular peptides described above could be included in such composite systems.

Another important challenge towards the use bioinspired materials with tailored bulk mechanical properties for tissue engineering applications will be to design materials that present appropriate biophysical and biochemical cues to direct cell fate or function at the nanoscale. Integrin binding cell adhesion ligands are necessary for the survival of many cell types, and the altered density and type of cell adhesion ligands coupled to biomedical materials can profoundly influence the resulting cell fate and behavior [109]. In addition to integrin binding ligands, tethered growth factors can also modulate the functionality of implanted scaffolds. Indeed, recent work has demonstrated that the tethering of high affinity growth factors to fibrin gels can be used to enhance bone regeneration and wound healing [110]. In addition to biochemical cues, biophysical cues such as material stiffness can impact various cellular behaviors. For example, mesenchymal stem cells undergo osteogenic differentiation optimally in ionically cross-linked alginate matrices with an elastic modulus of 10 – 30 kPa, and adipogenesis in gels with a modulus of 1 – 10 kPa [109]. On the other hand, no effect of stiffness is observed when MSCs are encapsulated in covalently cross-linked gels, with adipogenesis occurring over a range of elastic moduli of 4 – 90 kPa [111]. In these gels, osteogenesis only occurs when the gel is engineered to be degradable by cellular enzymes, demonstrating the additional importance of crosslinking type and degradability on stem cell fate. Research efforts such as those described above highlight how nanoscale tuning of the biochemical and biophysical environment of polymeric scaffolds can be utilized to promote desired outcomes in the context of tissue engineering. Our ability to precisely manipulate hybrid materials at the molecular scale by integrating some of the designs discovered in natural systems adds an extra dimension to this tailorability, similar to modular concepts previously used to confer multi-functionality of bioelastomers [112] and other soft materials [113]. For example, one can imagine incorporating the coiled coil heptad repeats from snail egg capsules into other recombinant protein constructs in order to mimic the high stiffness, elasticity, and energy absorption associated with the reversible α-β phase transition. Similarly, the modular sequence design of SRT could be exploited in several ways to achieve novel performance metrics. Specifically, the nanoconfined β-sheet forming modules from SRT could be used to control the relative content of the β-sheet reinforcement phase in hybrid biopolymers, and in turn, their mechanical response. In addition, photo-induced di-tyrosine cross-linking could also be used to modulate the mechanical properties of recombinant suckerin-based materials over several orders of magnitude.

7. Conclusions

The diversity of biomaterials employed for biomedical applications (synthetic, natural, and hybrid systems) have been expanding rapidly in recent years, with many developments in areas such as cell recognition, controlled degradation, or mechanical tuning. The molecular design of natural materials provide countless design lessons to chemists and materials scientists, at all length

scales of their structural hierarchy, to further improve the mechanical performance and expand the multi-functionality of their synthetic analogs. Until recently, elucidating the sequences of intriguing model proteinaceous materials, which constitutes a prerequisite for many molecular-based biomimicry approaches, was considered a challenging and time-consuming endeavor. Recent advances in NextGen sequencing technologies, however, have considerably reduced this time constraint, while at the same time, high-throughput sequencing costs are now a fraction of what they were just five years ago. Taken together, they point to the remarkable potential of vast libraries of biological materials waiting to be elucidated, and whose properties could fill up the empty materials properties landscape, particularly if one is able to recapitulate them in artificial systems using polymer synthesis and/or protein engineering approaches. It is our view that curiosity-driven discoveries of intriguing biological systems, combined with a keen eye towards the biological function of model tissues and careful multi-scale characterization all the way down to the molecular level, holds high potential to discover a wide range of novel materials with potential usage in tissue engineering and regenerative medicine applications.

Acknowledgements

We thank Dr. Paul Guerette (NTU) and Dr. Shawn Hoon (A*STAR, Singapore) for insightful comments and discussions during the preparation of this manuscript. A.M. acknowledges financial support from the Singapore National Research Foundation (NRF) through a NRF Fellowship, and the Singapore Ministry of Education (MOE) for a Tier 2 grant (grant # MOE 2011-T2-2-044) supporting the sucker ring teeth work.

References

1. P. Y. Chen, J. McKittrick and M. A. Meyers, *Progress in Materials Science*, 2012, **57**, 1492-1704.
2. S. Amini and A. Miserez, *Acta Biomateriala*, 2013, **9**, 7895–7907.
3. M. A. Meyers, J. McKittrick and P. Y. Chen, *Science*, 2013, **339**, 773-779.
4. J. Dunlop, R. Weinkamer and P. Fratzl, *Materials Today*, 2010, **14**, 70-78.
5. C. Guo and M. Spector, in *Scaffolding in Tissue Engineering*, eds. P. X. Ma and J. H. Elisseeff, CRC Press, Taylor&Francis group, Boca Raton, FL, 2006, pp. 385-411.
6. R. Lanza, R. Langer and J. Vacanti, eds., *Principles of Tissue Engineering*, Third edn., Elsevier Academic Press, Burlington, MA, 2007.
7. E. A. Sander and V. H. Barocas, in *Collagen: Structure and Mechanics*, ed. P. Fratzl, Springer-US, New York, 2008, pp. 475-504.
8. L. E. R. O'leary, J. A. Fallas, E. L. Bakota, M. K. Kang and J. D. Hartgerink, *Nature Chemistry*, 2011, **3**, 821-828.
9. F. G. Omenetto and D. Kaplan, *Science*, 2010, **329**, 528-531.

10. M. Ehrbar, S. C. Rizzi, R. Hlushchuk, V. Djonovb, A. H. Zisch, J. A. Hubbell, F. E. Weber and M. P. Lutolf, *Biomaterials*, 2007, 3856-3866.
11. N. Annabi, S. M. Mithieux, G. Camci-Unal, M. R. Dokmeci, A. S. Weiss and A. Khademhosseini, *Biochemical Engineering Journal*, 2013, **77**, 110-118.
12. N. A. Peppas, J. Z. Hilt, A. Khademhosseini and R. Langer, *Advanced Materials*, 2006, **18**, 1345–1360.
13. M. P. Lutolf and J. A. Hubbell, *Nature Biotechnology*, 2005, **23**, 47–55.
14. C. J. Kearney and D. J. Mooney, *Nature Materials*, 2013, **12**, 1004–1017.
15. O. A. Ali, N. Huebsch, L. Cao, G. Dranoff and D. J. Mooney, *Nature Materials*, 2009, **8**, 151–158.
16. C. Storm, J. J. Pastore, F. C. MacKintosh, T. C. Lubensky and P. A. Janmey, *Nature*, 2005, **435**, 191-194.
17. A. E. X. Brown, R. I. Litvinov, D. E. Discher, P. K. Purohit and J. W. Weisel, *Science*, 2009, **325**, 741-744.
18. J. R. Houser, N. E. Hudson, L. Ping, E. T. O'Brien, R. Superfine, S. T. Lord and M. R. Falvo, *Biophysical Journal*, 2010, **99**, 3038–3047.
19. W. F. McKay, S. M. Peckham and J. M. Badura, *Int. Orthop.*, 2007, **31**, 729–734.
20. C. A. Simmons, E. Alsberg, S. Hsiong, W. J. Kim and D. J. Mooney, *Bone*, 2004, **35**, 562–569.
21. L. S. Nair and C. T. Laurencin, *Progress in Polymer Science*, 2007, **32**, 762-798.
22. P. Fratzl, K. Misof, I. Zizak, G. Rapp, H. Amenitsch and S. Bernstorff, *Journal of Structural Biology*, 1998, **122**, 119-122.
23. A. A. Jalan and J. D. Hartgerink, *Current Opinion in Chemical Biology*, 2013, **17**, 960-967.
24. H. S. Gupta, in *Collagen: Structure and Mechanics*, ed. P. Fratzl, Springer-US, New York, 2008, pp. 155-173.
25. T. J. Wess, in *Collagen: Structure and Mechanics*, ed. P. Fratzl, Springer-US, New York, 2008, pp. 49-80.
26. S. V. Madihally and H. W. Matthew, *Biomaterials*, 1999, **20**, 511-521.
27. L. Q. Wu, R. Ghodssi, Y. A. Elabd and G. F. Payne, *Advanced Functional Materials*, 2005, **15**, 189-195.
28. M. Benjamin, H. Toumi, J. R. Ralphs, G. Bydder, T. M. Best and S. Milz, *Journal of Anatomy*, 2006, **208**, 471-490.
29. H. L. Lu and S. Thomopoulos, *Ann. Rev. Biomed. Eng.*, 2013, **15**, 201-226.
30. A. Miserez, T. Schneberk, C. Sun, F. W. Zok and J. H. Waite, *Science*, 2008, **319**, 1816-1819.
31. K. U. Claussen, T. Scheibel, H.-W. Schmidt and R. Giesa, *Macromol. Mater. Eng.*, 2012, **297**, 938-957.
32. J. D. Fox, J. R. Capadona, P. D. Marasco and S. J. Rowan, *J Am Chem Soc*, 2013, **135**, 5167-5174.
33. M. F. Ashby, *Materials Selection and Process in Mechanical Design*, 3rd edn., Butterworth Heinemann, Oxford, UK, 2005.
34. U. Wegst and M. F. Ashby, *Philosophical Magazine*, 2004, **84**, 2167-2181.
35. P. X. Ma and J. H. Elisseeff, *Scaffolding in Tissue Engineering*, CRC Press, 2006.
36. J. M. Gosline, M. A. Lillie, E. Carrington, P. Guerette, C. Ortlepp and K. Savage, *Philosophical Transactions of the Royal Society of London, Series B: Biological Sciences*, 2002, **357**, 121-132.
37. S. Lv, D. M. Dudek, Y. Cao, M. M. Balamurali, J. Gosline and H. Li, *Nature*, 2010, **465**, 69-73.
38. X. Zhao, *Soft Matter*, 2014, **10**, 672-687.
39. T. L. Sun, T. Kurokawa, S. Kuroda, A. Bin Ihsan, T. Akasaki, K. Sato, A. H., T. Nakajima and J. P. Gong, *Nature Materials*, 2013, **12**, 932-937.

40. A. Miserez, Y. Li, J. H. Waite and F. Zok, *Acta Biomateriala*, 2007, **3**, 139-149.
41. A. Miserez, S. Wasko, C. Carpenter and J. H. Waite, *Nature Materials*, 2009, **8**, 910 - 916.
42. A. Miserez, Y. Li, J. Cagnon, J. C. Weaver and J. H. Waite, *Biomacromolecules*, 2012, **12**, 332-341.
43. H. S. Rapoport and R. E. Shadwick, *Biomacromolecules*, 2002, **3**, 42-50.
44. H. S. Rapoport and R. E. Shadwick, *Journal of Experimental Biology*, 2007, **210**, 12-26.
45. P. A. Guerette, G. Z. Tay, S. Hoon, J. J. Loke, A. F. Hermawan, C. N. Z. Schmitt, M. J. Harrington, A. Masic, A. Karunaratne, H. S. Gupta, K. S. Tan, A. Schwaighofer, C. Nowak and A. Miserez, *Biomaterials Science*, 2014, **2**, 710-722.
46. M. J. Harrington, S. Wasko, A. Masic, F. D. Fisher, H. S. Gupta and P. Fratzl, *Journal of the Royal Society Interface*, 2012, **9**, 2911-2922.
47. A. Miserez and P. A. Guerette, *Chem. Soc. Rev.*, 2013, **42**, 1973-1995.
48. A. Zhmurov, O. Kononova, R. I. Litvinov, R. I. Dima, V. Barsegov and J. W. Weisel, *J Am Chem Soc*, 2012, **134**, 20396–20402.
49. Z. Qin and M. J. Buehler, *Physical Review Letters*, 2010, **104**, 198304.
50. I. Schwaiger, C. Sattler, D. R. Hostetter and M. Rief, *Nature Materials*, 2002, **1**, 232-235.
51. J. B. Addison, N. N. Ashton, W. S. Weber, R. J. Stewart, G. P. Holland and J. L. Yarger, *Biomacromolecules*, 2013, **14**, 1140–1148.
52. N. N. Ashton, D. R. Roe, R. B. Weiss, T. E. Cheatham and R. J. Stewart, *Biomacromolecules*, 2013, **14**, 3668-3681.
53. A. Miserez, J. C. Weaver, P. B. Pedersen, T. Schneberk, R. T. Hanlon, D. Kisailus and H. Birkedal, *Advanced Materials*, 2009, **21**, 401-406.
54. P. A. Guerette, S. Hoon, D. Ding, S. Amini, A. Masic, B. Venkatesh, V. Ravi, J. C. Weaver and A. Miserez, *ACS Nano*, 2014.
55. P. A. Guerette, S. Hoon, Y. Seow, F. T. Wong, V. H. B. Ho, M. Raida, A. Masic, M. C. Demirel, F. Abdon, S. Amini, G. Z. Tay, D. Ding and A. Miserez, *Nature Biotechnology*, 2013, **31**, 908–915.
56. J. H. Waite and M. Tanzer, *Science*, 1981, **212**, 1038-1040.
57. J. H. Waite, T. J. Housley and M. L. Tanzer, *Biochemistry*, 1985, **24**, 5010-5014.
58. K. J. Coyne, X. X. Qin and H. Waite, *Science*, 1997, **277**, 1830-1832.
59. J. H. Waite and X.-X. Qin, *Biochemistry*, 2001, **40**, 2887-2893.
60. H. Zhao and J. H. Waite, *Biochemistry*, 2006, **45**, 14223-14231.
61. J. Yu, W. Wei, E. Danner, R. K. Ashley, J. N. Israelachvili and J. H. Waite, *Nature Chemical Biology*, 2011, **7**, 588-590.
62. P. L. Lee, P. B. Messersmith, J. N. Israelachvili and J. H. Waite, *Annual Reviews of Materials Research*, 2011, **41**, 99-132.
63. J. Sedó, J. Saiz-Poseu, F. Busqué and D. Ruiz-Molina, *Advanced Materials*, 2012, **25**, 653-701.
64. H. Lee, S. M. Dellatore, W. M. Mille and P. B. Messersmith, *Science*, 2007, **318**, 426-430.
65. J. O. Warwicker, *Acta Crystallographica*, 1954, **7**, 565-573.
66. M. Xu and R. V. Lewis, *Proceedings of the National Academy of Sciences of the United States of America*, 1990, **87**, 7120-7124.
67. P. A. Guerette, D. Ginzinger, B. Weber and J. M. Gosline, *Science*, 1996, **272**, 112-115.
68. C. Y. Hayashi and R. Lewis, *Science*, 2000, **287**, 1477-1479
69. J. Gatesy, C. Y. Hayashi, D. Motriuk, J. Woods and R. Lewis, *Science*, 2001, **291**, 2603-2605.
70. C. C. Broomell, R. K. Khan, D. N. Moses, A. Miserez, M. G. Pontin, F. W. Zok and J. H. Waite, *Proceedings of the Royal Society Interface*, 2007, **4**, 19-31.
71. S. A. Andersen, *Insect Biochem Mol Biol*, 2010, **40**, 166-178.
72. D. Rubin, A. Miserez and J. H. Waite, in *Advances in Insect Physiology*, ed. J. Casas, Elsevier, 2010, vol. 38, pp. 75-133.

73. H. Ellegren, *Trends in Ecology & Evolution*, 2014, **29**.
74. M. L. Metzker, *Nat. Rev. Genet.*, 2009, **11**, 31-46.
75. Z. Wang, M. Gerstein and M. Snyder, *Nat. Rev. Genet.*, 2009, **10**, 57-63.
76. F. Ozsolak and P. M. Milos, *Nat. Rev. Genet.*, 2011, **12**, 87-98.
77. M. G. Grabherr, B. J. Haas, M. Yassour, J. Z. Levin, D. A. Thompson, I. Amit, X. Adiconis, F. L., R. Raychowdhury, Q. Zeng, Z. Chen, E. Mauceli, N. Hacohen, A. Gnirke, N. Rhind, F. Di Palma, B. W. Birren, C. Nusbaum, K. Lindblad-Toh and F. N., *Nature Biotechnology*, 2011, **29**, 644-652.
78. Z.-F. Chen, K. Matsumura, H. Wang, S. M. Arellano, X. Yan, I. Alam, J. A. C. Archer, V. B. Bajic and P. Y. Qian, *PLoS One*, 2011, **7**, e22913.
79. B. Lengerer, R. Pjeta, J. Wunderer, M. Rodrigues, R. Arbore, L. Schärer, E. Berezikov, M. W. Hess, K. Pfaller, B. Egger, S. Obwegeser, W. Salvenmoser and P. Ladurner, *Frontiers in Zoology*, 2014, **11**, 1-15.
80. E. Hennebert, R. Wattiez, M. Demeuldre, P. Ladurner, D. S. Hwang, J. H. Waite and P. Flammang, *Proceedings of the National Academy of Sciences of the United States of America*, 2014, **111**, 6317–6322.
81. S. Gomes, I. B. Leonor, J. F. Mano, R. L. Reis and D. L. Kaplan, *Progress in Polymer Science*, 2011, **37**, 1-17.
82. B. D. Olsen, *AIChE J.*, 2013, **59**, 3558-3568.
83. R. V. Lewis, *Chemical Reviews*, 2006, **106**, 3762−3774
84. M. Delorenzi and T. Speed, *Bioinformatics*, 2002, **18**, 617-625.
85. C. T. Armstrong, T. L. Vincent, P. J. Green and D. N. Woolfson, *Bioinformatics*, 2011, **27**, 1908-1914.
86. S. Wasko, G. Tay, C. Nowak, A. Schwaighofer, J. H. Waite and A. Miserez, *Biomacromolecules*, 2014, **15**, 30−42.
87. H. Herrmann, H. Bär, L. Kreplak, S. V. Strelkov and U. Aebi, *Nature Reviews Molecular Cell Biology*, 2007, **6**, 562-573.
88. M. Arslan, Z. Qin and M. J. Buehler, *Computer Methods in Biomechanics and Biomedical Engineering*, 2011, **14**, 483-489.
89. O. J. L. Rackham, M. Madera, C. T. Armstrong, T. L. Vincent, D. N. Woolfson and J. Gough, *Journal of Molecular Biology*, 2010, **403**, 480-493.
90. B. Apostolovic, D. Maarten and H.-A. Klok, *Chem. Soc. Rev.*, 2010, **39**, 3541-3575.
91. J. M. Gosline, P. A. Guerette, C. S. Ortlepp and K. N. Savage, *Journal of Experimental Biology*, 1999, **202**, 3295– 3303.
92. Z. Z. Shao and F. Vollrath, *Nature*, 2002, **418**, 741-741.
93. H. Tao, D. L. Kaplan and F. G. Omenetto, *Advanced Materials*, 2012, **24**, 2824-2837.
94. J. Zhang, E. Pritchard, X. Hu, T. Valentin, B. Panilaitis, F. G. Omenetto and D. L. Kaplan, *Proceedings of the National Academy of Sciences of the United States of America*, 2012, **109**, 11981-11986.
95. X. X. Xia, Z. G. Qian, C. S. Ki, Y. H. Park, D. L. Kaplan and S. Y. Lee, *Proceedings of the National Academy of Sciences of the United States of America*, 2010, **107**, 14059-14063.
96. T. Weis-Fogh, *Journal of Molecular Biology*, 1961, **3**, 648-667.
97. C. M. Elvin, A. G. Carr, M. G. Huson, J. M. Maxwell, R. D. Pearson, T. Vuocolo, N. E. Liyou, D. C. C. Wong, D. J. Merritt and N. E. Dixon, *Nature*, 2005, **437**, 999-1002.
98. P. M. Kharkar, K. L. Kiick and A. M. Kloxin, *Chem. Soc. Rev.*, 2013, **42**, 7335-7372.
99. J.-Y. Sun, X. Zhao, W. R. K. Illeperuma, O. Chaudhuri, K. H. Oh, D. J. Mooney, J. J. Vlassak and Z. Suo, *Nature*, 2012, **489**, 133-136.
100. O. Chaudhuri, S. T. Koshy, C. Branco da Cunha, J.-W. Shin, C. S. Verbeke, K. H. Allison and D. J. Mooney, *Nature Materials*, 2014.

101. L. Han, A. J. Grodzinsky and C. Ortiz, *Annual Review of Materials Research*, 2011, **41**, 133–168.
102. D. J. Huey, J. C. Hu and K. A. Athanasiou, *Science*, 2012, **338**, 917-921.
103. A. H. Huang, M. J. Farrell and R. L. Mauck, *Journal of Biomechanics*, 2010, **43**, 128–136.
104. K. Ma, A. L. Titan, M. Stafford, C. H. Zheng and M. E. Levenston, *Acta Biomaterialia*, 2012, **8**, 3754–3764.
105. M. Guo, L. M. Pitet, H. M. Wyss, M. Vos, P. Y. W. Dankers and E. W. Meijer, *J Am Chem Soc*, 2014, **136**, 6969–6977.
106. E. Ducrot, Y. Chen, M. Bulters, R. P. Sijbesma and C. Creton, *Science*, 2014, **344**, 186-189.
107. D. S. Fudge, K. H. Gardner, V. T. Forsyth, C. Riekel and J. M. Gosline, *Biophysical Journal*, 2003, **85**, 2015-2027.
108. C. W. Wolgemuth and S. X. Sun, *Physical Review Letters*, 2006, **97**, 248101.
109. N. Huebsch, P. R. Arany, A. S. Mao, D. Shvartsman, O. A. Ali, S. A. Bencherif, J. Rivera-Feliciano and D. J. Mooney, *Nature Materials*, 2010, **9**, 518-526.
110. M. M. Martino, P. S. Briquez, E. Güç, F. Tortelli, W. W. Kilarski, S. Metzger, J. J. Rice, G. A. Kuhn, R. Müller, M. A. Swartz and J. A. Hubbell, *Science*, 2014, **343**, 885-888.
111. S. Khetan, M. Guvendiren, W. R. Legant, D. M. Cohen, C. S. Chen and J. A. Burdick, *Nature Materials*, 2013, **12**, 458–465.
112. L. Li, M. Charati and K. L. Kiick, *Polymer Chemistry*, 2010, **1**, 1160-1170.
113. A. M. Kushner and Z. Guan, *Angewandte Chemie, International Edition in English*, 2011, **50**, 9026-9057.

Figure legends

Figure 1. Tensile stress-strain curves of representative soft biomaterials used in medical applications (top: linear stress scale; bottom log stress scale). Between the stiff silks and (native and cross-linked) collagens and the more compliant bioelastomers and hydrogels (which exhibit a higher strain to failure), there are limited materials with properties that fall between these boundaries.

Figure 2. Materials selection charts of representative soft biomaterials. **(a)** Strain to failure *vs.* elastic modulus of soft biomaterials, with blue dotted lines denoting the guidelines along which materials exhibit an equivalent strain energy to failure. **(b)** Characteristic tensile response of materials featuring a mechanical hysteresis during load cycles. The total elastic energy stored at peak stress corresponds to the full area under the curves, whereas the internally-absorbed mechanical energy during a load cycle corresponds to the colored areas. **(c)** Ashby Plot of total hysteresis *vs.* elastic modulus. Yellow areas in **(a)** and **(c)** correspond to the "empty soft materials space", in which limited biocompatible soft materials are found. Marine snail egg capsules and caddisfly silks are found within these areas.

Figure 3. An integrative approach combining Next Gen sequencing (RNA-seq) with proteomics and materials characterization for the discovery of novel molecular designs and architectures for the development of new biomimetic materials. Adapted from Ref. (55).

Figure 4. Ashby plot of H vs. E of common engineering materials along with recombinant suckerin (Rec-suckerin 39, wet conditions) after cross-linking. Rec-suckerin exhibits very high elastic modulus and hardness that can compete with the best structural synthetic polymers, with the final properties depend on the di-tyrosine cross-link density. Such material could find usage in restorative biomedical applications requiring high load-bearing capability. Reproduced from Ref. (55).

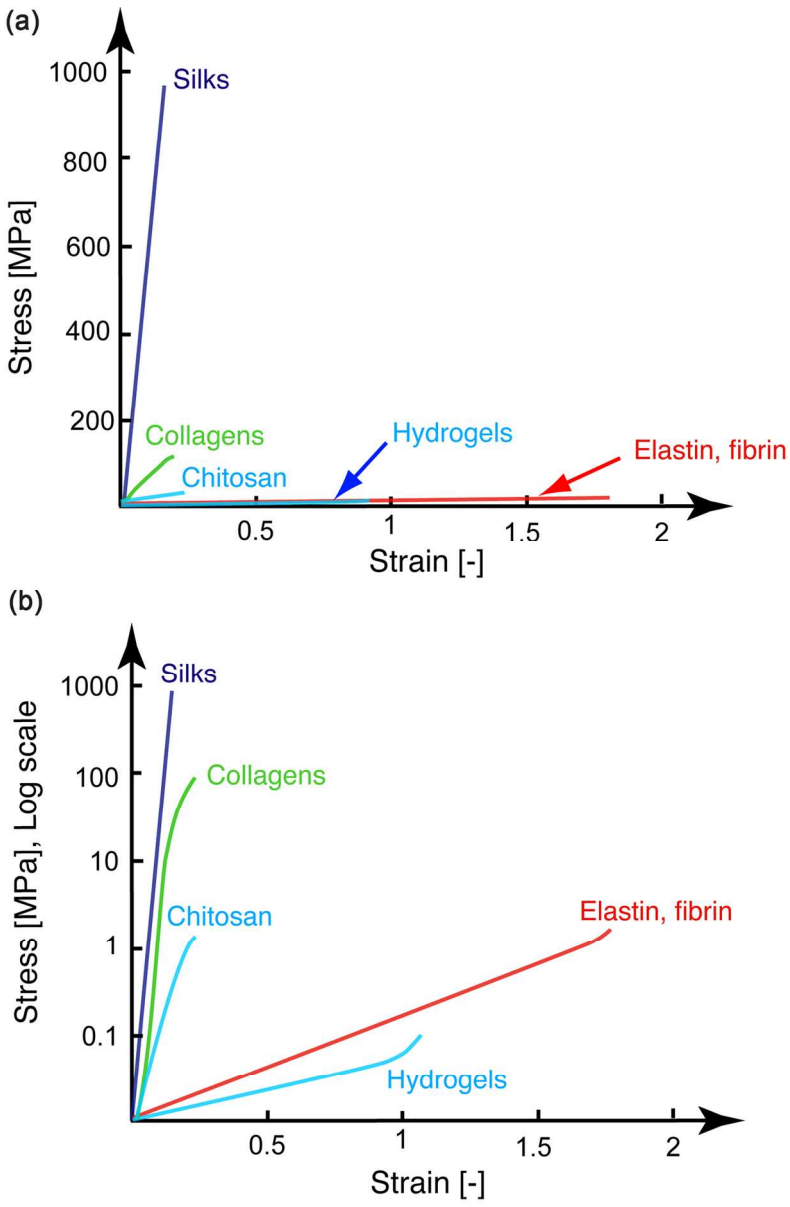

119x183mm (300 x 300 DPI)

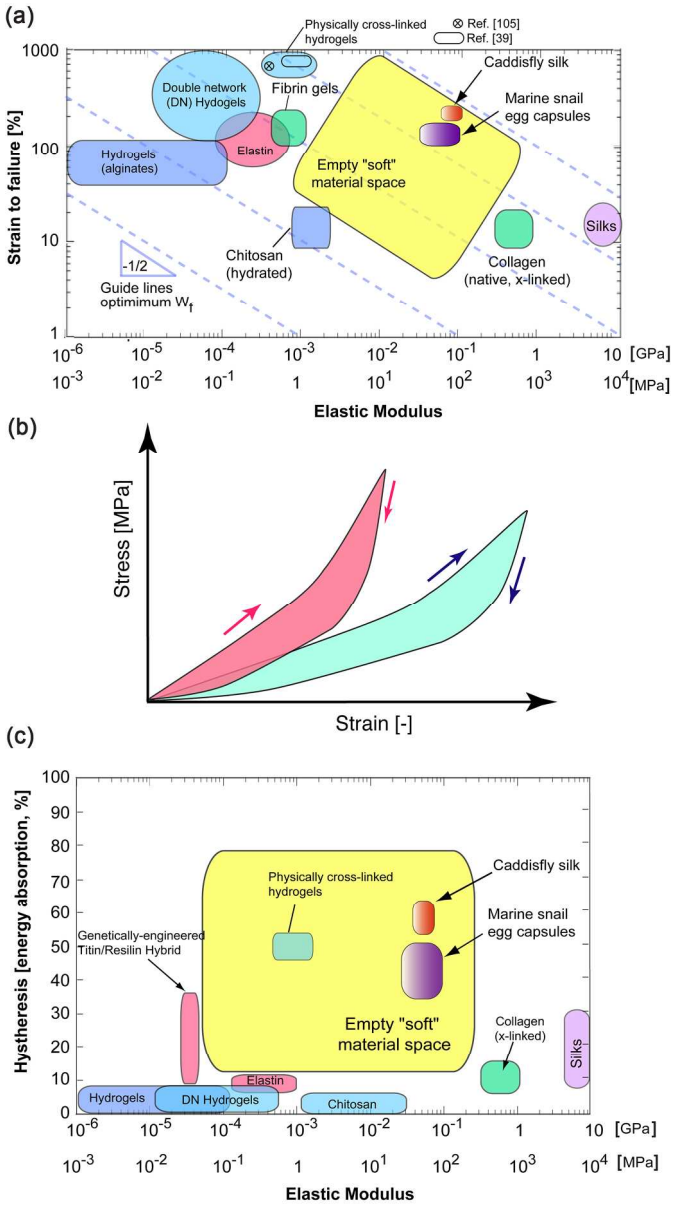

180x324mm (300 x 300 DPI)

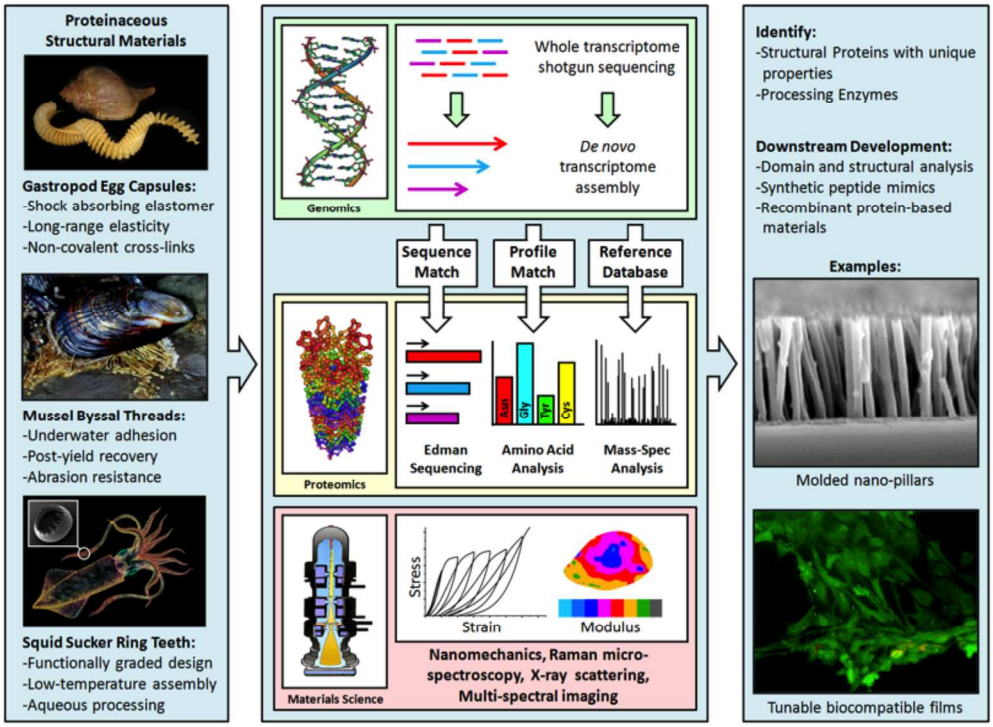

219x160mm (300 x 300 DPI)

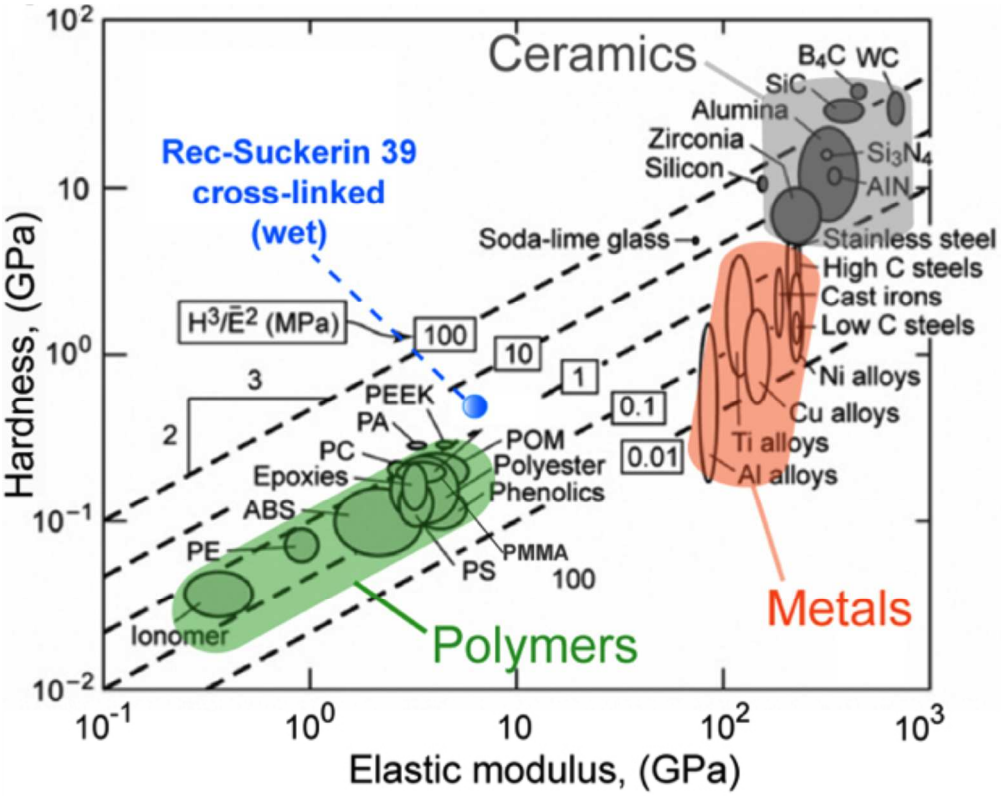

199x158mm (300 x 300 DPI)